# SAMPLE QUANTITY PRODUCTION OF ULTRA-HIGH REFRACTIVE INDEX DISTRIBUTIONS OF GLASS MICROSPHERES

**by**

**Clark G. Kuney Jr.**

**A Research Paper**

**Submitted in Partial Fulfillment of the**

**Requirements for the**

**Masters of Science Degree**

**in**

**Management Technology**

**Approved 4 Semester Credits**

______________________________

**Research Advisor**

**The Graduate School**

**University of Wisconsin-Stout**

**April, 2003**

The Graduate School

University of Wisconsin Stout

Menomonie, WI 54871

**ABSTRACT**

| Kuney | Clark | G |
| --- | --- | --- |
| (Last Name) | (First) | (Initial) |

Sample Quantity Production of Ultra-High Refractive Index Distributions of Glass
(Title of Thesis)

Microspheres

Management Technology
(Graduate Major)

| Dr. Rajiv Asthana | April, 2003 | 37 |
| --- | --- | --- |
| (Research Advisor) | (Date) | (No. of Pages) |

Publication Manual of the American Psychological Association.-5th ed.
(Manual Style)

Street and highway signs are made from a layered retroreflective material fastened to an aluminum back plate. The retroreflective material uses microspherical glass lenses, commonly called glass beads, as the active optical element. These glass beads have a refractive index of either 1.9 or 2.2. Owing to product construction constraints, a glass bead of 2.9 refractive index would allow products to be developed having improved brightness, simplified construction, and longer sign life. The research presented here involved the preparation of sample quantities of glass beads ranging from 2.5 to 2.9 refractive index from proprietary formulations. The scope of this experiment was limited to crucible batching and melting, hand crushing and screening, and small scale forming into microspheres. The glass crushing and forming equipment was constructed from common farm and laboratory apparatus. Finally, the retroreflective property of the 2.9

refractive index beads produced was demonstrated in a simple product simulation. The author of this research, Clark G. Kuney Jr. is also the author of U.S. Patent Number 4,957,335 titled “Microsphere-based Retroreflective Articles With Enhanced Retroreflective Brightness” and is considered a past authority on the subjects of both microsphere formulations and processing.

# Table of Contents

## Author Note: Proprietary Information

Because the goal of this research is to produce materials in support of a patent application, the glass formulations and certain other proprietary information have been purposely omitted. Were they included, they would constitute Premature Disclosure and void any patent rights obtained.

List of Tables

## List of Figures

# Chapter One

## Introduction

Street and highway signs are made from a layered retroreflective material fastened to an aluminum back plate. The retroreflective material uses microspherical glass lenses, commonly called glass beads, as the active optical element. These glass beads have a refractive index of either 1.9 or 2.2. Owing to product construction constraints, a glass bead of 2.9 refractive index would allow products to be developed having improved brightness, simplified construction, and longer sign life.

This paper begins with a brief review of retroreflective signing material and glass beads. It details why a 2.9 refractive index bead would be a major improvement and how the associated products would be constructed. It then documents the laboratory efforts that will be used to produce sample quantities of these beads. Finally, the results of the laboratory work and further recommendations will be presented. The goal of the research is to produce sample quantities of nominal 2.9 refractive index beads for use in obtaining a patent.

### Background and Significance

The availability of 2.9 refractive index beads would make possible a new class of retroreflective signing material. That material is expected to be up to 67% brighter than its premium competitive product line, have a much longer life span, and be cheaper to produce. The resulting economic benefits to the consumer and the safety benefits to the motoring public are therefore substantial.

## Research Delimitations

The research will be limited to the production of sample quantities of beads and a rudimentary demonstration of their retroreflective capabilities. No attempts will be made to fabricate finished sheeting or to optimize the bead making process.

## Assumptions

The Department of Transportation has long called for brighter signing material in an effort to make driving at night safer. It is assumed this situation has not changed.

The author first produced these beads while employed in the field. It is assumed that the employer has not continued development nor patented the composition.

No other technology has been developed that would supplant the usefulness of a signing system based on 2.9 refractive index beads.

## Definitions of Terms

*Retroreflection.* Light striking a surface and returning back into the medium in the reverse direction (i.e., a 180 degree change from its original path). (Micropat.com, 2003) As used in signing material, retroreflection occurs when the light from the headlights of an auto strike a sign, and are returned in a cone of illumination. This cone is large enough to include the driver's eyes, thus allowing him/her to see the sign at night.

*Refractive index.* $n = c / v$ where: $n$ = refractive index

$c$ = velocity of light in a vacuum

$v$ = velocity of light in the material

(Flinn & Trojan, 1975)

The refractive index (RI) of a material is the property that indicates the degree to which light is deflected or bent when entering a material of a different index. A common example would be the apparent “bending” of a stick as it is immersed at an angle in water.

# Chapter Two

## Literature Review

The first known appearance of retroreflective sheeting occurred in the 1940's. It was an exposed lens variety. Sheeting technology has advanced over the years to an enclosed lens, wide angle flat top, and finally to a micro replicated product based on cube corner design. Each of these products has been an advancement, yet each has contained product limitations. This section will document the basic sheeting types and their limitations while illustrating why 2.9 refractive index bead based products would be superior. This is followed by a discussion of bead size and refractive index distributions and their effect on optical properties. Finally, references are given for contemporary product websites.

### Patents

*Exposed Lens.*

Gebhard, Heltzer, Clarke, and Davis (1943) obtained the first U.S. patent on a retroreflective product. It was an exposed lens type of sheeting as depicted here.

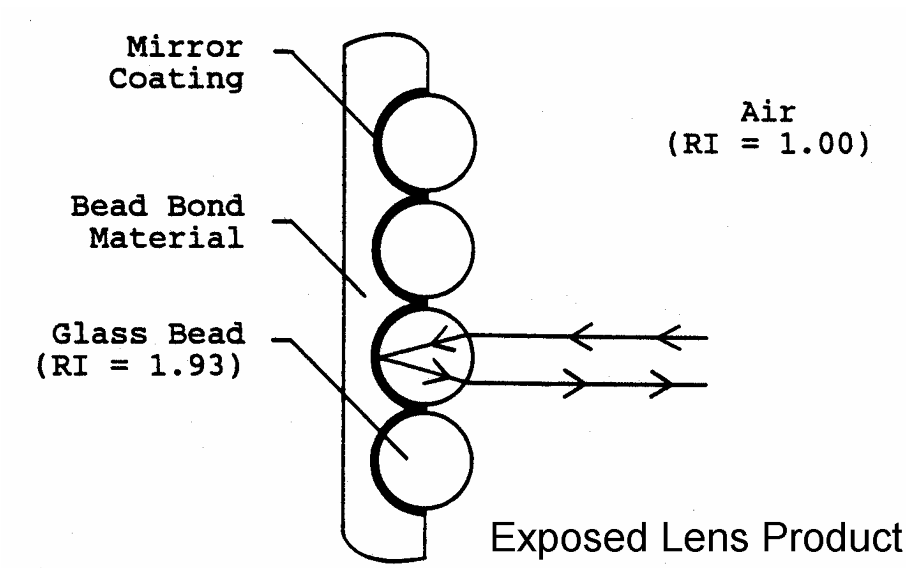


(Geo-Stellar, 1992)

Kuney (1990, pg. 1) states:

> "One drawback of exposed-lens type of construction is that if the surface of the … sign becomes wet, … the water … interferes with the desired retroreflection, thereby "blacking out" the affected sheeting."

This basic design flaw led to two separate solutions, encapsulated lens sheeting and wide angle flat top sheeting.

*Encapsulated Lens.*

McKenzie (1965) obtained the first patent for an encapsulated sheeting type of product.

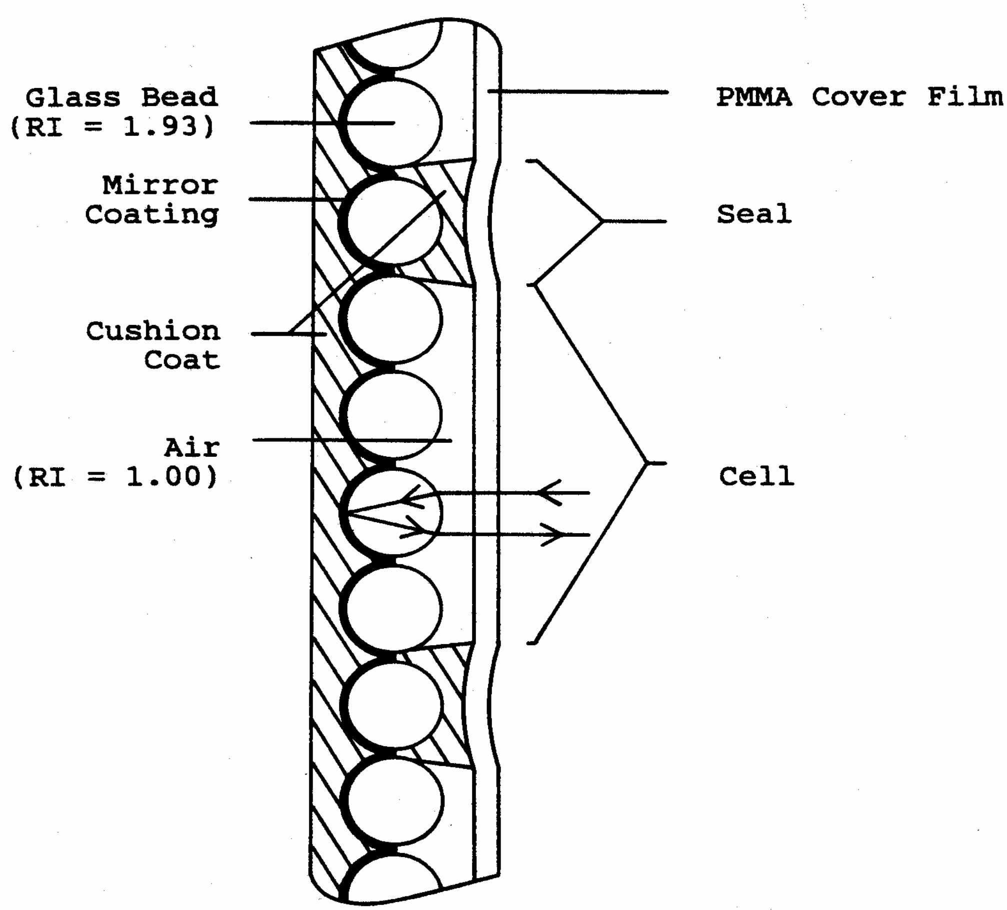


Encapsulated Lens Product

(Geo-Stellar, 1992)

Variations of this type of sheeting remain in wide use as premium signing material. Yet this product suffers from two flaws. The first is the necessity to seal the Cover Film to the Cushion Coat. This effectively reduces the retroreflecting surface area of the sign. The second flaw is that the air space between the Cover Film and the Glass Beads traps water and contaminates that attack and destroy the beads. Encapsulated sheeting is also relatively expensive to manufacture.

*Wide Angle Flat Top.*

Wide Angle Flat Top (WAFT) type sheeting is in common use and is a compromise solution between the exposed and encapsulated products.

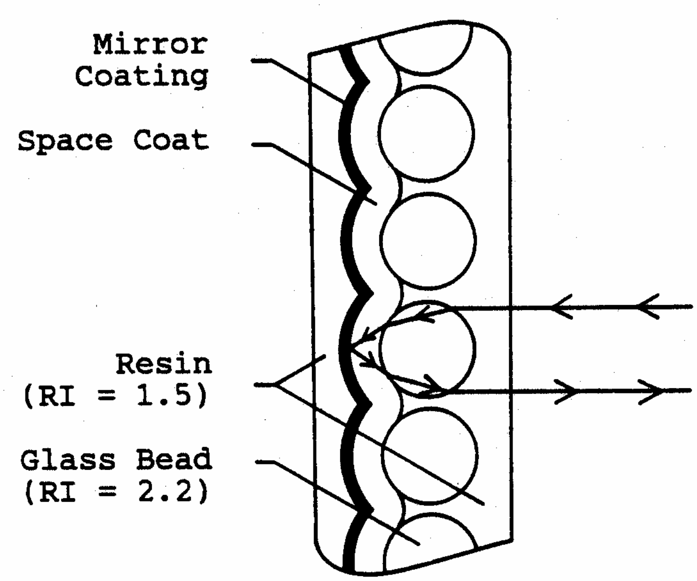


WAFT Product

(Geo-Stellar, 1992)

It is relatively cheap to produce and fully protects the beads. However, it suffers from lower brightness and weatherability, both due to the necessity of the Space Coat. As Tung and Laird (1980) indicate, the space coat is necessary because “the art has never … provided commercially useful glass microspheres having a refractive index higher than about 2.7." Tung and Laird go on to detail how increasing the refractive index of the beads will cause the thickness of the Space Coat to decrease and that the availability of a 2.9 refractive index bead would make possible a WAFT type product without a spacecoat.

*Proposed 2.9 Wide Angle Flat Top.*

This research will produce 2.9 refractive index beads for use in a Proposed 2.9 WAFT type of sheeting.

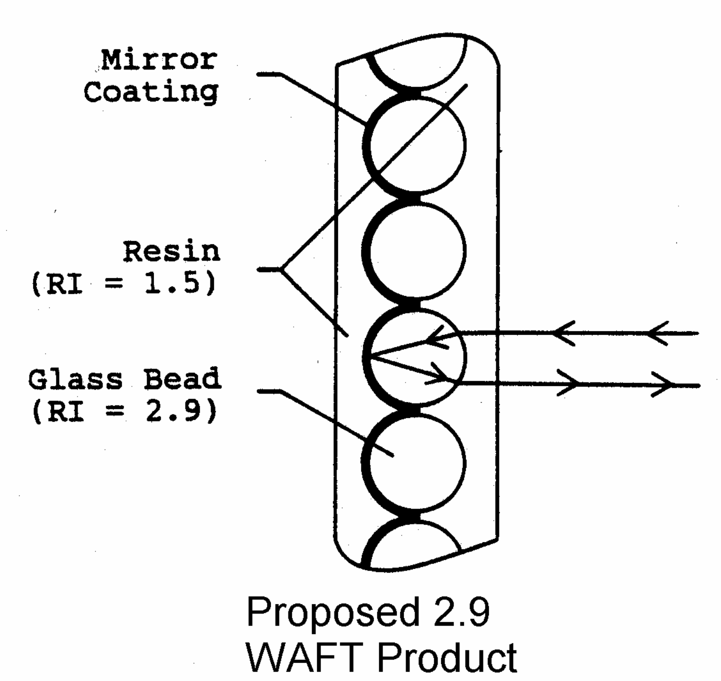


(Geo-Stellar, 1992)

As Geo-Stellar (1992) documents, this type of sheeting is expected to have the following properties:

| | Encapsulated Lens | Current WAFT | Proposed 2.9 WAFT |
|---|---|---|---|
| Brightness (Cd/Lux/$m^2$) | 300-570* | 100 | 500-920* |
| Cost Relative to Current WAFT | 2.5x | 1.00x | .89x |
| Weatherability | Good | Fair | Excellent |

* The higher values can only be achieved by using the technology described by Kuney (1990).

Sheeting Comparison Table

Bead Distributions

In his seminal work on the relationships between bead sizes, brightness, and refractive index, Kuney (1990) taught that both the average bead size and the standard deviation of the bead size distribution have dramatic impacts on the optical properties of the resulting products. Kuney also demonstrated that nominal 1.9 refractive index beads produce useful retroreflection at indices as low as 1.87 when average 55µ beads are used and as high as 2.05 when used with beads averaging 160µ in diameter. Thus a new class of "focused" encapsulated sheeting was predicted and demonstrated by the production of "high contrast" signing systems.

The processing of glass beads necessarily produces both bead size and refractive index distributions. Characterized by average and standard deviation measurements like any normal distribution, they arise for the following reasons. Size distributions are produced when the beads or particles are screened. This phenomena is well documented and understood. Refractive index distributions arise from the variable compositional and thermal histories of beads as they are batched and formed. That is, particles have very slight differences in composition after batching and melting. Later, they experience different melting/freezing profiles as the particles pass through different parts of the former flame. This adds to the compositional variation by burning off different amounts of low refractive index flux materials. The differences in the melting/freezing profiles also produce differences in density that impacts refractive index.

So it becomes clear that references to beads of a size and refractive index are actually referencing beads of a size distribution having a refractive index distribution. The control of these distributions and the matching of them with the desired product functionality was Kuney's (1990) contribution to the art.

In the context of the current research, production of a 2.9 refractive index bead is understood to mean the production of beads having both a size distribution and a refractive index distribution including 2.9. Further, the exact refractive index to target is not knowable until the entire optical component of the final product (i.e.; the refractive index of the enclosing resin or plastic) is defined. That is, first one defines the product construction (based on performance, cost and weathering criteria) and then formulates the bead to match the system. Thus it is much more useful to demonstrate that the subject glass formulations may be adjusted over a broad refractive index range than to prove that an exact refractive index average can be produced.

Contemporary Product References

3M is the acknowledged market leader in retroreflective products. Their excellent web sites are referenced as the definitive current embodiments of the retroreflective products.

*Encapsulated Sheeting.*

Marketed as High Intensity$^{TM}$ sheeting, a number of product variations are available. Their web site is:

http://products3.3m.com/catalog/us/en001/safety/traffic_control/node_GSLB4QWKB8be/root_GST1T4S9TCgv/vroot_1PGXVVLN9Xge/gvel_4KN1JV2791gl/theme_us_trafficcontrol_3_0/command_AbcPageHandler/output_html

*WAFT Sheeting.*

Marketed as Engineer Grade$^{TM}$ sheeting, a number of product variations are available. Their web site is: http://products3.3m.com/catalog/us/en001/safety/traffic_control/node_GSQ2WQWVQDbe/root_GST1T4S9TCgv/vroot_1PGXVVLN9Xge/gvel_4KN1JV2791gl/theme_us_trafficcontrol_3_0/command_AbcPageHandler/output_html

*Cube Corner Sheeting.*

A relatively new and extremely premium product is now available. It is based on the use of micro retroreflective cube corned depressions. Marketed as Diamond Grade$^{TM}$ sheeting, a number of product variations are available. Their web site is: http://products3.3m.com/catalog/us/en001/safety/traffic_control/node_KHS6XW8TBJbe/root_GST1T4S9TCgv/vroot_1PGXVVLN9Xge/gvel_4KN1JV2791gl/theme_us_trafficcontrol_3_0/command_AbcPageHandler/output_html

# Chapter Three

## Methodology

### Batching

*Formulations.*

Five separate batches were prepared. They were:

| Batch # | Targeted Refractive Index |
|---|---|
| 1 | 2.472 |
| 2 | 2.87 |
| 3 | 2.900 |
| 4 | 3.104 |
| 5 | 2.702 |

Table Of Batches

*Calculation of Refractive Index.*

The targeted refractive index was calculated on a molar weight basis. A simple spreadsheet was written to facilitate the batch calculation. It was based on the formula:

$$\frac{(M * RI)_{RM1} * (M * RI)_{RM2} * \cdots\cdots * (M * RI)_{RMn-1} * (M * RI)_{RMn}}{M_{RM1} + M_{RM2} + \cdots\cdots + M_{RMn-1} + M_{RMn}} = TRI$$

where:

M = moles

RI = Refractive Index as given by Perry and Chilton (1973)

RM# = Raw Material Number

n = Number of Different Raw Materials

TRI = Targeted Refractive Index

*Calculation of Melt Temperatures.*

The projected batch melting temperature was also calculated on a molar weight basis. The spreadsheet was based on the formula:

$$\frac{(M * T)_{RM1} * (M * T)_{RM2} * \cdot\cdot\cdot\cdot\cdot * (M * T)_{RMn-1} * (M * T)_{RMn}}{M_{RM1} + M_{RM2} + \cdot\cdot\cdot\cdot\cdot + M_{RMn-1} + M_{RMn}} = PBMT$$

where:

M = moles

T = Raw Material Melting Temperature as given by Perry and Chilton (1973)

RM# = Raw Material Number

n = Number of Different Raw Materials

PBMT = Projected Batch Melting Temperature

*Procedure.*

The raw materials (RM) were weighed using an Ohaus Digital Scale Model GT2100. Each RM was carefully weighed and then added to a 5" mortar. After all the RMs were batched, they were ground together using a pestle until no trace of individual particles was evident.

<u>Melting and Cooling</u>

The resulting batch was then placed in a Coors 100 ml High Form High Alumina crucible. The crucible and batch were then melted in the upper chamber of a Cress Electric Furnace Model C2121 at a temperature between 100 and 200 °F higher than the PBMT. Following a 30-minute soak at temperature, the furnace heaters were turned off while the circulating fan continued to run. The furnace was then allowed to cool for 20 minutes before the crucibles were removed to air. After cooling to room temperature, the crucible and its glass were then broken up for further processing.

Initial Break Up

The crucible was placed in a plastic bag inside of a paper bag. A hammer was used to break up the crucible and glass into small pieces. The crucible pieces were then removed and the glass crushed.

Construction of the Glass Crusher

Crushing the glass pieces using a mortar and pestle proved ineffective, so a glass crusher was made from a ¾" Top Link Ball and Pin. See the Appendix for a photograph of the Glass Crusher.

Operation of the Glass Crusher

The glass pieces were placed in the crusher chamber between the base and the pin. The entire unit was then placed in a Carver Model M Hydraulic Press and a load of up to 10,000 pounds was applied.

*Screening of the Glass.*

The crushed glass was then screened using 8" Tyler Sieves to a –200 / +325 mesh (-75µ / +45µ) particle size distribution. The +200 mesh material was recrushed and rescreened until sufficient samples were obtained.

Construction of the Flame Former

The basic former body was constructed from a DOT 17H 30 Gallon Steel Drum.

*Construction of the Burner System.*

The burner system used to melt and form the glass particles into spheres was constructed from a Meker natural gas burner. Initial tests using very small quantities of hand feed particles were successful, but subsequent attempts to automate the feeding of particles developed two problems:

1) The flame became unstable at the grid due to the feed system placing the gas and air mixture into turbulent flow.

2) The heat produced by the burner was not adequate to melt the increased quantity of particles.

Both of these problems were solved by adding a 10” extension to the burner body. This returned the gas & air mixture to a laminar flow, thus allowing much larger quantities to be burned. In turn this produced the heat necessary to melt the increased quantities of particles. See the Appendix for a photograph of the Burner System.

*Construction of the Feeder System.*

An automated feeder system was constructed from an Elite Model 801 aquarium air pump, a plastic test tube, a two-holed stopper, ¼” plastic hose, and 3/16” stainless steel brake line tubing. The air pump forced air through the tubing into the test tube where it fluidized the glass particles. A second tube carried the fluidized particles to the burner feed distribution tube. The rate of flow was controlled by adjusting the distance between the intake tube end and the feed material. That is, as the intake tube was moved closer to the bottom of the test tube and the particles, more of them became fluidized and picked up by the exhaust tube. See the Appendix for a photograph of the Feeder System and a Close Up Of The Feeder System Test Tube.

*Construction of the Feed Distribution Tube.*

The feeder system connected to a feed distribution tube within the body of the burner. The tube was designed to produce an even particle distribution across the cross section of the burner body tube. This was necessary to ensure a relatively consistent thermal history for all beads by evenly loading the former flame. See the Appendix for a photograph of the Feed Distribution Tube.

Operation of the Flame Former with the Feeder System

Because the flame former was built with out instrumentation, its operation was based on experience. After lighting the burner and establishing a steady flame, the feed system was adjusted to give a slow but steady rate. The initial material produced was viewed under 100x magnification. This evaluation was used to adjust the feed rate and flame size until acceptable product was being produced. The former was then cleaned and the actual run begun. After approximately 1 hour, the former was shut down and the beads were collected.

Two chronic problems developed during use. The first was the presence of water and oil in the gas line, which contaminated the former and caused it to smoke. This required the termination of two of the three former runs. The second was the susceptibility of the feed system to clogging due to humidity. This was handled by frequently tapping the feed line until it was cleared.

Screening of the Former Product

The former product was passed through a 200 mesh (-75µ) Tyler Sieve to remove scale and combustion product residue. The –200 mesh material was weighed on the Ohaus Digital Scale and became the final sample.

Demonstration of Retroreflection

A proper demonstration of retroreflection in a reasonable product optical system was far beyond the scope of this experiment. However, a crude product optical system, sufficient to demonstrate retroreflection, was constructed by the following means. The sample beads were placed in a small vial. A piece of Scotch™ tape was placed over the vial mouth. After the vial was inverted and righted, the excess beads were tapped loose and the tape removed. It carried a circular monolayer of beads on its adhesive side. The tape was then allowed to pick up a small piece of aluminum foil, shinny side towards the beads. The tape/beads/foil package was then pressed onto a glass slide for stability while handling. The entire slide was then vigorously rubbed over its tape surface to force the beads through the adhesive layer and to force the aluminum foil to conform to the curve of the beads. See the Appendix for a photograph of the Retroreflective Slide Demonstration.

In this crude system, the tape acts as the plastic surface of the product. The adhesive layer is ignored (a serious flaw for this optical system) and the aluminum foil acts as a reflective layer. Any air layer between the beads and the foil is also ignored.

The demonstration consists of viewing the slide at an angle while illuminating it with a small flashlight. The flashlight is initially held to one side and then slowly rotated into the same line of sight as the observers. That is, the flashlight butt is placed against the observer's nose. As the illumination and line of sight coincide, some of the beads could be seen to become a bright and shinny gray. This is the light being retroreflected by the optical system back towards the flashlight.

# Chapter Four

## Results and Discussion

### Batching and Melting

Of the five melts attempted, only three were successful. They produced glass targeted at refractive indexes of 2.472, 2.702, and 2.900. The results were:

| Batch # | Targeted Refractive Index | Results |
|---|---|---|
| 1 | 2.472 | Good melt, successful |
| 2 | 2.87 | Crucible failed; batch lost |
| 3 | 2.900 | Good melt, successful |
| 4 | 3.104 | Failed, unknown reaction product |
| 5 | 2.702 | Good melt, successful |

Table Of Batch Results

### Crushing and Screening

Use of the glass crusher was very successful. Each of the three glass samples was repeatedly crushed and screened using 8" Tyler Sieves to a –200 / +325 mesh (-75µ / +45µ) size distribution until several hours of former feed was collected. Samples of the uncrushed glass were also retained. See the Appendix for a photographs of the Crushed Glass Particles at 100x and 200x.

### Flame Forming and Screening

Approximately 1.5 grams of each of the three glass samples were obtained. Microscopic examination at 100x showed these samples were approximately 75% beads and 25% unformed particles. Only about ¼ of each supply of former feed was actually processed. The balances were stored as samples.

Batch #1 was used to initially configure the former. It was from these results that it became clear that the burner system required modification as described on pages 13-14.

After modification, Batches #1,3, and 5 were each processed. The forming for Batches #1 and 3 took about 1 hour and produced approximately 1.5 grams of finished sample. Batch #5 was processed at a higher rate, although this was not recognized at the time.

Batches #1 and 3 were actually terminated when the former began to smoke due to water and oil in the gas line entering the former. Batch #5 was terminated after 40 minutes simply because sufficient material had been run to obtain a sample of comparable size to #1 and 3. The former product was then screened through a 200 mesh Tyler Sieve and weighed. The results were:

| Batch # | Flame Former Run # | Forming Time (Hrs) | Sample Weight (Grams) |
|---|---|---|---|
| 1 | 4 | 1 | 1.58 |
| 3 | 1 | 1 | 1.51 |
| 5 | 1 | 40 minutes | 1.52 |

Table Of Former Results

See the Appendix for a photographs of the Glass Beads at 100x and 200x.

Demonstration of Retroreflection

Demonstration slides of all three samples were made. As expected, only the Batch #3 sample (Target Refractive Index = 2.9) showed significant true retroreflection. The others showed the characteristic “warm” appearance of systems near but off optical compliance for retroreflection.

# Chapter Five

# Summary and Conclusions

## General

This experiment successfully produced beads of the targeted refractive index and demonstrated their retroreflective ability. Further, it demonstrated that the subject glass system is capable of producing beads from –2.5 to +2.9 refractive index as needed. And while this experiment was delimited to the production of samples without any effort being made to optimize the bead making process, still a number of processing recommendations can be made.

## Batching and Melting

The use of non-high alumina crucibles would substantially reduce the experimental costs, but their compatibility with this glass system would need to be determined.

The use of the Cress Electric Furnace proved somewhat problematic due to its large size and lack of view port. A rapid rise crucible furnace capable of obtaining the necessary temperatures would make the melting of samples much easier.

Further research is needed to resolve the melting characteristics of Batch #4.

## Crushing and Screening

The glass crusher that was fabricated worked very well in conjunction with the Carver Hydraulic Press. However, a larger glass crusher, possibly 2” in diameter would facilitate processing and remove the necessity for initial break up of the glass chunks.

Hand screening with the Tyler Sieves was very effective.

## Feeding and Flame Forming

The flame former as constructed and modified with its burner system worked very well. Its operation, while dependent on experience and not on instrumentation, proved fairly reliable and reproducible. The fluidized feeder system proved more problematic due to lack of instrumentation and susceptibility to humidity. A number of former and feeder recommendations are possible, however their implementation would require significant resources.

1) Increasing the grid diameter from 1 ½” to 8” would reduce the percentage of unformed particles.

2) Separate, metered air and gas lines would allow for more reproducibility in the flame conditions and operation.

3) An oil and water trap on all air and gas lines would prevent former contamination and smoking.

4) An automated collection system would facilitate sample collection.

5) A metered feed system would reduce product variation and help insure reproducibility of results.

## Demonstration of Retroreflection

The crude Demonstration Slides prepared functioned adequately, but contain a number of optical flaws that limit their real world value. Production of product samples (e.g.; sheeting samples) from typical materials would facilitate both the demonstration of retroreflection and the optimization of batch composition and processing to achieve maximum brightness. However, product sample production requires extensive experience, equipment and materials.

Direct Measurement Of Bead Refractive Index

No accepted, direct measurement technique for measuring the refractive index of beads in the 2.5 to 2.9 range exists. However, the author is aware of a proposal to develop such a test based on known optical properties. This test should be developed and validated as part of the general effort to bring 2.9 refractive index bead based products to market.

# References


Flinn, R. A. & Trojan, P. K. (1975). *Engineering Materials And Their Applications.* Boston: Houghton Mifflin Company.

Gebhard, M. L., Helzer, H., Clarke, J. E., & Davis, E.P. (1943). *U.S. Patent No. 2,326,634*. Washington, DC: U.S. Patent and Trademark Office.

Geo-Stellar (1992). *Funding Proposal For Retroreflective Products.* (Available from the Geo-Stellar Corporation, 708 Mifflin Street, Philadelphia, PA 19148)

Kuney, C. G. (1990). *U.S. Patent No. 4,957,335*. Washington, DC: U.S. Patent and Trademark Office.

McKenzie, E. L. (1965). *U.S. Patent No. 3,190,178*. Washington, DC: U.S. Patent and Trademark Office.

Micropat.com website (2003). *Definition of Retroreflection.* Retrieved March 26, 2003 from http://www.micropat.com/classdef/CLSDEF/class359/s000000.html.

Perry, R. H., & Chilton, C. H. (1973). *Chemical Engineers' Handbook* (5th ed.) New York: McGraw-Hill.

Tung, C. F. & Laird, J. A. (1980). *U.S. Patent No. 4,192,576*. Washington, DC: U.S. Patent and Trademark Office.

Appendix

**Glass Crusher**


**Burner System**


**Feeder System**

**Close Up Of The Feeder System Test Tube**

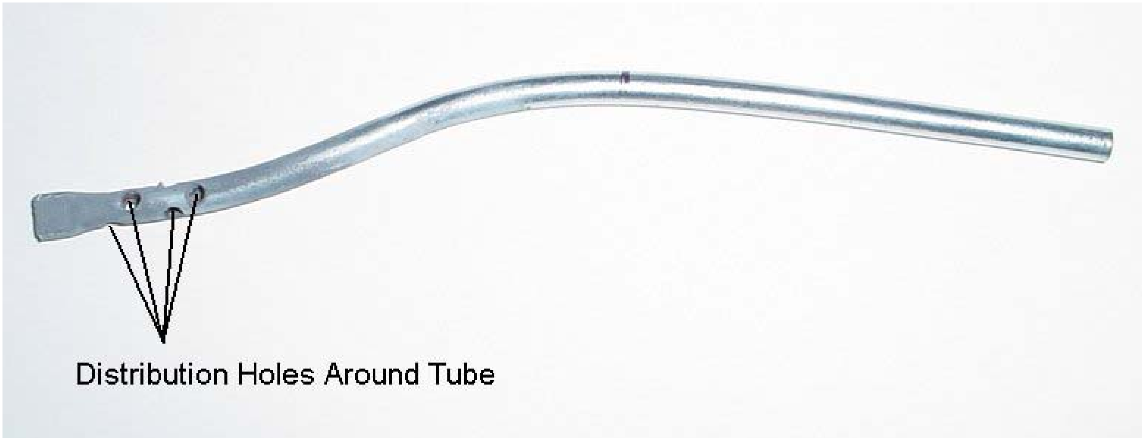


**Feed Distribution Tube**

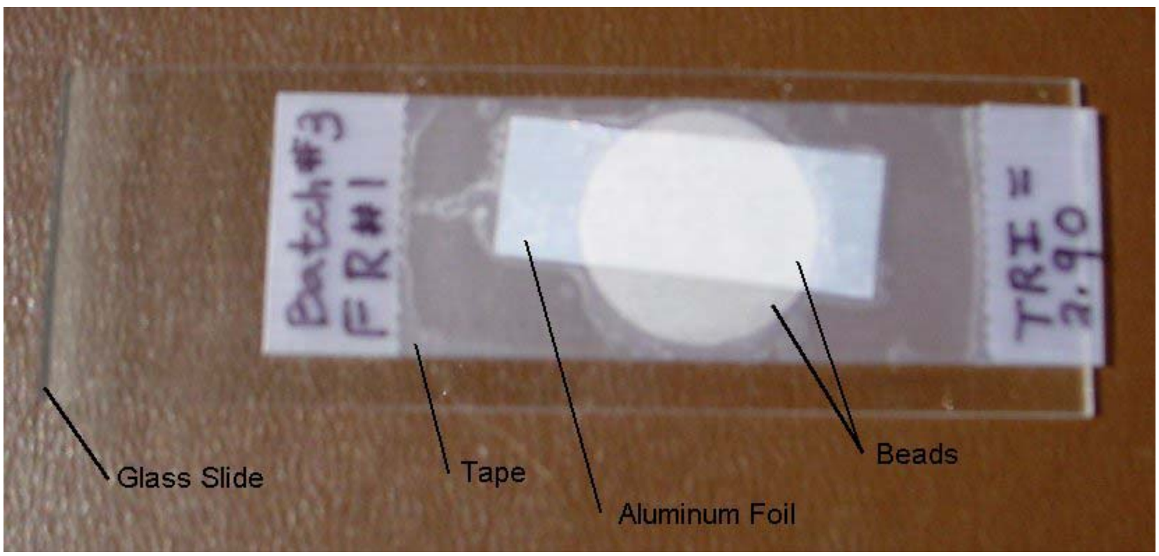


**Retroreflective Slide Demonstration**

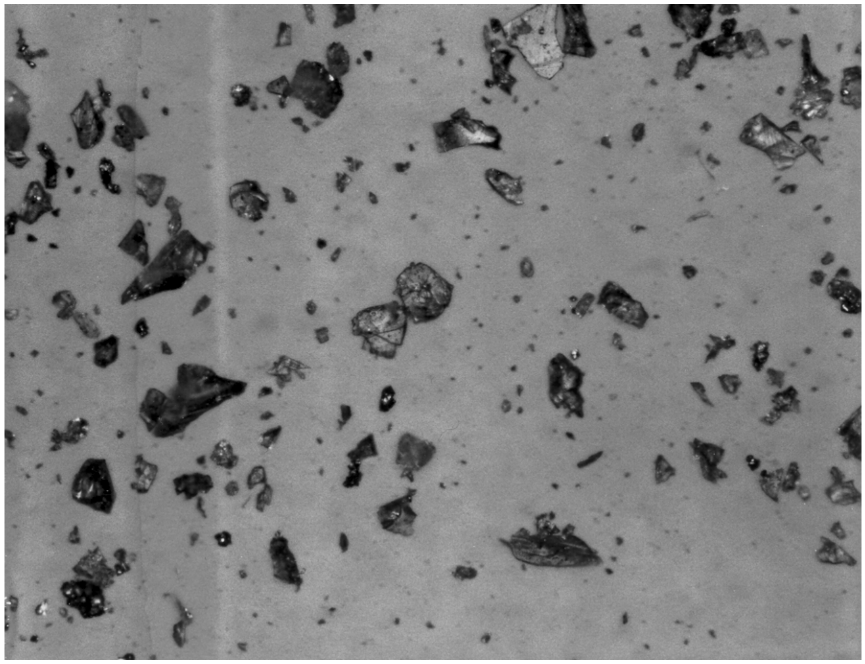

**Crushed Glass Particles at 100x**

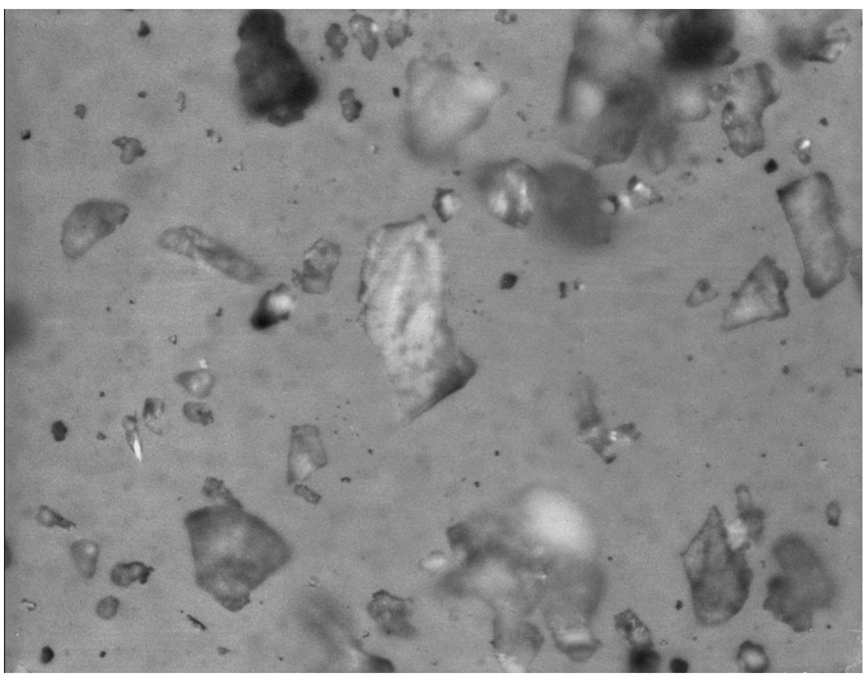

**Crushed Glass Particles at 200x**

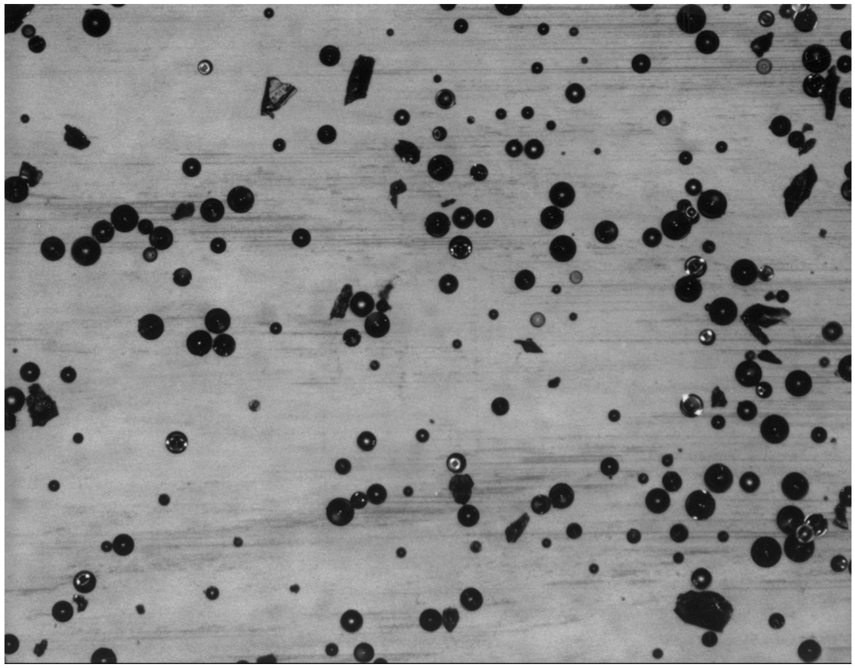

**Glass Beads at 100x**

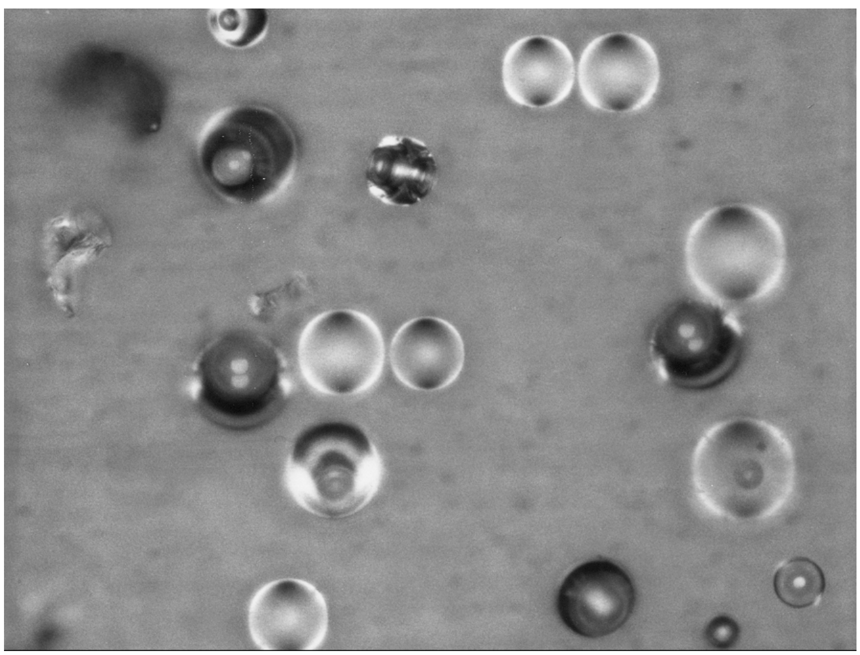

**Glass Beads at 200x**